Replacing the nucleus pulposus of the intervertebral disk: prediction of suitable properties of a replacement material using finite element analysis

J. R. MEAKIN, D. W. L. HUKINS
Department of Biomedical Physics and Bioengineering, University of Aberdeen, Foresterhill, Aberdeen, AB25 2ZD, UK

An axisymmetric finite element model of a human lumbar disk was developed to investigate the properties required of an implant to replace the nucleus pulposus. In the intact disk, the nucleus was modeled as a fluid, and the annulus as an elastic solid. The Young's modulus of the annulus was determined empirically by matching model predictions to experimental results. The model was checked for sensitivity to the input parameter values and found to give reasonable behavior. The model predicted that removal of the nucleus would change the response of the annulus to compression. This prediction was consistent with experimental results, thus validating the model. Implants to fill the cavity produced by nucleus removal were modeled as elastic solids. The Poisson's ratio was fixed at 0.49, and the Young's modulus was varied from 0.5 to 100 MPa. Two sizes of implant were considered: full size (filling the cavity) and small size (smaller than the cavity). The model predicted that a full size implant would reverse the changes to annulus behavior, but a smaller implant would not. By comparing the stress distribution in the annulus, the ideal Young's modulus was predicted to be approximately 3 MPa. These predictions have implications for current nucleus implant designs.

1. Introduction

The purpose of this paper is to predict suitable properties for an implant to replace the nucleus pulposus (abbreviated to ''nucleus'') which forms the inner region of the intervertebral disk. In the intact disk, the gel-like nucleus is contained within the fibrous layers of the annulus fibrosus (abbreviated to ''annulus'') [1, 2]. Some surgical procedures for the treatment of low back pain involve removal of part of the nucleus [3–5]. This removal may involve using lasers [6] or injection of an enzyme [7].

Removal of the nucleus has been shown to change the response of the annulus to compression [8–10]. In the intact disk, both the inner and outer margins of the annulus bulge outwards under compression. However, when the nucleus is removed, the direction of bulging of the inner margins changes towards the center of the disk. The implication of these changes is that the shear stresses between the lamella of the annulus will tend to increase [11], possibly leading to circumferential tears, which are a sign of disk degeneration [12, 13]. A possible solution to this potential problem may be to replace the nucleus with a suitable synthetic implant.

Currently at least eleven nucleus implant designs have been granted US patents, but little published research has investigated their suitability. The main aim of these implants appears to be to restore disk height and flexibility [14]. However, it may also be important to design implants which will address the problem of changes to the response of the annulus.

A finite element (FE) model was developed to provide general information on how an implant would affect this response, and to predict suitable properties for an implant material. FE techniques have been used to model the response of the disk to applied loads since the 1970s [15]. Many models have incorporated increasing detail to represent an individual disk, rather than disks as a whole. However, they may then predict some atypical feature of that disk [16]. In order to design an implant, it was necessary to predict how it would behave in all disks.

All modeling attempts to represent reality, whilst simplifying the system so that it is easier to understand [17]. It is thus necessary to define what aspect of the system is important. In this study it is the direction of bulging of the annulus margins. The simplest possible model is then to consider the disk as a cylindrical nucleus surrounded by an annulus which is a thick cylindrical shell; the same approximation has been made previously in an analytical model to investigate the functions of the components of the disk [18]. A cylindrical FE model has a further advantage in that the axisymmetry of the system can be exploited to simplify the analysis and, hence, reduce the computation time [19].

2. Methods

2.1. Intact disk model

The model of a disk was developed using ANSYS revision 5.2 (ANSYS Inc., Houston, PA, USA) running on a Sparcstation 5 (Sun Microsystems, Inc., Palo Alto, CA, USA). The geometry of the intervertebral disk was approximated to be cylindrical as shown in Fig. 1. This approximation meant that the geometry could be described in terms of just three parameters: height, H, disk radius, R_d, and nucleus radius, R_n. This geometrical simplification allowed the full three-dimensional model to be created in two dimensions, using axisymmetric element types. Thus the model was created using areas which are considered by the software to be equivalent to the cylindrical volume they would create if they were rotated 360° about the cylinder axis, which defines the y-axis in Fig. 2. Exploiting axisymmetry, rather than describing the model in three dimensions, means a finer, and hence more accurate, mesh can be applied without a great increase in computation time [19].

The model of the intact disk is shown in Fig. 2. The area on the left represents the nucleus and the area on the right represents the annulus. The element types used in the model were two-dimensional, 4 node, axisymmetric elements. The nucleus was modeled as a fluid using FLUID81 elements [20], since it interacts with the annulus by exerting a radial pressure [18]. The annulus was modeled as a homogeneous, isotropic, elastic solid using PLANE25 elements [20], to avoid the need to model its internal fibrous structure.

The dimensions of the model are given in Table I. These values were derived from measurements of the cross-sectional area of a whole human L5/S1 disk and its nucleus. Values were assigned to R_d and R_n to produce a model with the same areas. The height, H, of the model was equal to the mean height of the same disk. Although only one disk was used, comparison with values given in the literature [21–23] showed that the values were reasonable for a typical human lumbar disk.

The material properties assigned to the model are given in Table I. The bulk modulus of the nucleus was the mean value from measurements on non-degenerate or slightly degenerate nuclei from 17 human disks [24]. The value for Poisson's ratio of the annulus was taken to be the maximum value allowed by PLANE25 elements, i.e. 0.49. This value was chosen because an isotropic, homogeneous material which is incompressible, and hence undergoes no volume change under loading, will have a Poisson's ratio of 0.5 [25] for small strains. The annulus can be approximated to be an incompressible material since its is made up of 70% water [26, 27], which has a high bulk modulus. Further evidence to support this chosen value is given by experimental measurements in the range 0.46 to 1.63 [28].

The value for the Young's modulus of the annulus given in Table I was determined empirically by matching the output of the model to the experimental behavior of a real disk. This was done because the values reported in the literature ranged between approximately 0.1 and 1000 MPa [28–34]. This great variation appears to stem from the testing method used (compressive or tensile), the orientation of the annulus fibers to the applied load, the location from which the annulus sample was taken from the disk, and the variability between disks (biological variability or level of degeneration). Additionally, these values may not even be a true representation of the Young's modulus as the annulus samples tested were small; it has been shown that the stiffness of a small, isolated sample of annulus is less than that of the whole, intact annulus [35]. The determination of the Young's modulus is described in Section 2.2.

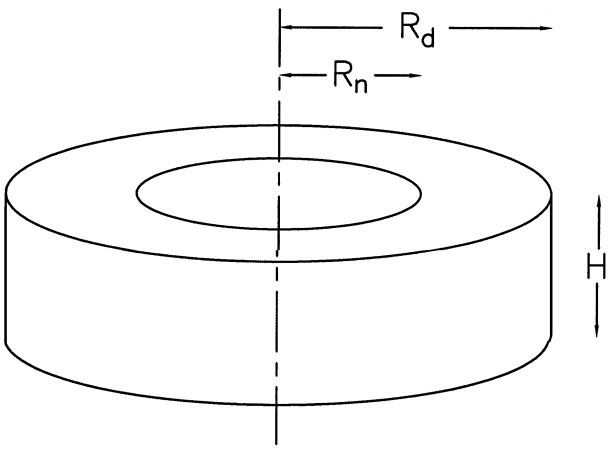

Figure 1 Geometry of intervertebral disk model, described by three dimensions: height of cylinder (H), radius of disk (R_d) and radius of nucleus (R_n).

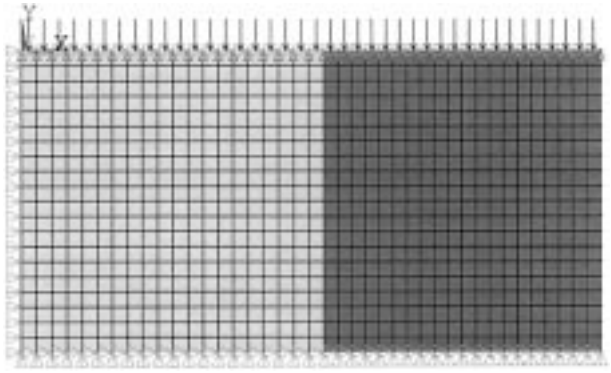

Figure 2 Model of the intact disk. The pale gray area on the left represents the nucleus, and the dark grey area on the right represent the annulus. The triangles along the top, left and bottom edges of the model represent applied constraints, and the arrows along the top represent the applied loading. The triad at the top left-hand corner of the model shows the origin and orientation of the Cartesian co-ordinate system used. The origin is the point of intersection of the cylinder axis with the upper surface of the model. The y-axis is defined by the cylinder axis, the x-axis lies in the radial direction and the z-axis completes the right-handed set.

TABLE I Material and geometrical properties of disk model

Dimension	Value
Height, H	12 mm
Disk radius, R_d	23 mm
Nucleus raidus, R_n	12 mm
Nucleus bulk modulus	1720 MPa
Annulus Poisson's ratio	0.49
Annulus Young's modulus	0.1–1000 MPa

All nodes were constrained in the z–direction (perpendicular to the plane of Fig. 2) to ensure the model stayed in the x–y plane (the plane of Fig. 2), a necessary condition for axisymmetry to be maintained. The nodes along the central axis were also constrained in the x-direction (radial direction) for the same reason. The nodes along the top and bottom of the model were constrained in the x-direction to represent the attachment of the disk to the end-plates and vertebral bodies. The nodes along the bottom of the model were constrained in the y-direction (axial direction) to represent a rigid and fixed lower vertebral body. The nodes along the top of the model were coupled in the y-direction. This was to represent the rigid but moveable upper vertebral body. All nodal constraints, other than those in the z-direction, are represented by triangles in Fig. 2.

Pressure was applied to the top of the model (represented by arrows in Fig. 2). The value of the pressure, P, was given by

$$P = \frac{F}{\pi \cdot R_d^2} \tag{1}$$

where F was a compressive load of 1.5 kN and R_d was the radius of the disk (23 mm). A load of 1.5 kN was used because it is within physiological range, but is expected not to result in fracture of the end-plates [36].

2.2. Determining the Young's modulus of the annulus

To determine a single value for the Young's modulus, the output of the model was compared to experimental results. The model output chosen for this purpose was the predicted axial displacement and bulging of the outer annulus margin. These were defined respectively as being the displacement of the top surface of the model in the y-direction, and the displacement of the mid-point of the right-hand edge of the model in the x-direction. Two human L5/S1 disks were tested to determine the axial displacement and outer annulus bulge under a compressive load of 1.5 kN. Compression was applied at a rate of 150 N s^{-1} using a testing machine (Instron 8511, Instron Corporation, Canton, MA, USA), and a lateral view of the disk was continuously recorded on to video tape. The axial displacement was calculated from the testing machine output, and the annulus bulge measured from the video images. The values obtained, and a comparison with the literature [37–40] showed that 1 mm was a good approximation to the real behavior for both axial displacement and outer annulus bulge.

The variation of axial displacement, and outer annulus bulge of the model, with Young's modulus from 1 to 10 MPa are shown in Fig. 3. For the model to match the behavior of a real disk, the Young's modulus of the annulus needed to give both an axial displacement and outer annulus bulge of approximately 1 mm. From the graph in Fig. 3 it was determined that a Young's modulus of 5 MPa would be the most suitable value to fulfil this condition.

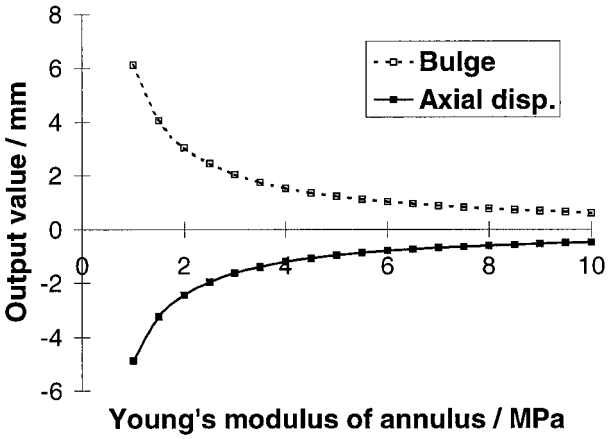

Figure 3 Predicted axial displacement (solid line and filled boxes) and outer annulus bulge (dotted line and hollow boxes) of the intact disk model for different values of annulus Young's modulus.

2.3. Validation

Validation for the model was obtained by comparing the behavior of the model to the experimental results obtained for intact and denucleated disks [8–10], and by performing sensitivity tests. The sensitivity tests took the form of varying the value of each input parameter individually. If changing the input caused the output to change unreasonably, then it could be said that that the input parameter was critical to the behavior of the model, and the value of that input parameter must be carefully chosen.

The deformed shape of the disk model with and without the nucleus is shown in Fig. 4. The predictions of

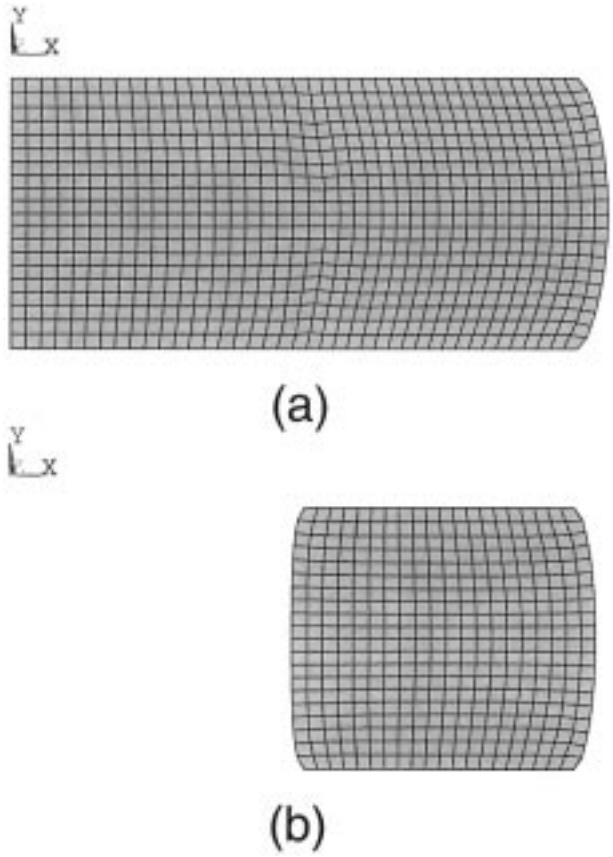

Figure 4 Deformed shape of the disk model: (a) nucleus present, (b) nucleus removed. Note that, unlike Fig. 2, the nucleus and the annulus in (a) are shown in the same color. The triads in the top left-hand corners show the origin and orientation of the co-ordinate system.

the model were that when the nucleus is present, the disk will reduce in height, and the annulus will deform by bulging outwards. When the nucleus is removed the model predicted that the inner regions of the annulus will bulge inwards. These predictions were consistent with the experimental results for intact and denucleated disks [8–10], showing that the disk model was valid to answer questions about subsequent replacement of the nucleus.

To see if choosing the Young's modulus, or any of the other input parameters had been critical to the model predictions, a sensitivity test was performed where each of the input parameters was varied individually. Table II shows the range over which each parameter was varied. The output which was assessed was the axial displacement and the outer annulus bulge. Table II also shows the range of output values which were obtained by varying each input parameter.

It can be seen from Table II, that neither the nucleus bulk modulus or the mesh size had any effect on the output values. Variation in applied load gave changes to output values as would be expected experimentally [37–39, 41]. Variation in the other input parameters also gave output values which were not unreasonable. More important, for the results of this study, is that none of the changes in input parameter values caused a sign change to the output, i.e. the axial displacement and the bulging of the outer annulus margin was always in the same direction.

2.4. Nucleus implant

An implant to replace the nucleus was modeled as an isotropic, homogeneous, elastic solid. The element type used was PLANE25, the same as had been used for the annulus. Two properties of the implant were investigated: its geometry (in terms of its radial size) and its material properties (in terms of its Young's modulus).

To investigate the effects of size, two different situations were considered, one where the implant was the same size as the cavity left by the removed nucleus (height 12 mm and radius 12 mm), and one where the implant was smaller than the cavity (height 12 mm and radius 11 mm). The two sizes are referred to as ''full size'' and ''small size'', respectively, in the remainder of this paper.

To investigate the effects of material properties, the Young's modulus of the implant was varied between 0.5 and 100 MPa. This range was chosen to encompass a reasonably large variety of polymeric materials. As the materials being considered were rubber-like, the Poisson's ratio of the implant was set at 0.49. This value, which is the highest value available with the PLANE25 element type, is reasonable for a rubber-like material [42].

Modeling the implant required modifications to be made to the model described in Section 2. In the intact disk model, the nucleus and the annulus shared a common boundary. However, an implant may not adhere to the annulus, requiring that it be modeled as having its own, separate boundary. To represent the interaction between the two separate components, CONTAC48 [20] elements were used. These are non-linear elements for modeling what happens when two surfaces come close to each other.

Another similar consideration was that, in the intact disk model, the top and bottom edges of the nucleus had been constrained radially (in the x-direction) to represent the attachment of the nucleus to the underlying end-plates. Again, an implant is unlikely to adhere to the end-plates, but will slide across them. The amount of sliding will be governed by the coefficient of friction between the two components. A search of the literature gave no satisfactory value for the coefficient of friction, so it was decided to consider two extreme cases: that of very high friction and that of zero friction. These situations were modeled by having either total or zero constraints on the nodes along the top and bottom edges of the implant.

3. Results

The typical deformed shape for the implants (full and small sized) are shown in Fig. 5. These examples are both for an implant with a Young's modulus of 5 MPa. Similar shapes of deformation were found for all the values of Young's modulus tested in both the high and zero friction cases, but with differences in deformation magnitude.

It can be seen from Fig. 5a that a full sized implant reverses the changes produced by denucleation (c.f. Fig. 4b). The smaller implant, though, is not so successful at returning the behavior of the annulus to that of the intact disk. The gap between the implant and the annulus allows them to deform independently. This means that the annulus bulges inwards (as in the denucleated disk) until such time as it makes contact with the implant, which is bulging outwards. It can be seen that where the two have bulged sufficiently for them to make contact,

TABLE II Input and output of sensitivity tests. The second column shows the range over which each parameter was varied, together with the value used in the model in brackets. The range of axial displacement and annulus bulge values obtained by varying each parameter are given in the third and fourth columns

Parameter	Input value range (model value)	Axial displacemmment range/mm	Annulus bulge range/mm
Annulus Poisson's ratio	0–0.49 (0.49)	−0.98–−1.94	0.36–1.22
Nucleus bulk modulus	920–2120 MPa (1720 MPa)	−0.98–−0.98	1.22–1.22
Height	2–14 mm (12 mm)	−0.02–−1.38	0.05–1.49
Radius of nucleus	10–18 mm (12 mm)	−0.92–−1.70	1.13–2.30
Radius of disk	19–29 mm (23 mm)	−2.10–−0.43	2.24–0.64
Load	0.5–2.5 kN (1.5 kN)	−0.33–−1.63	0.41–2.04
Total number of elements	72–3200 (800)	−0.93–−0.98	1.21–1.23

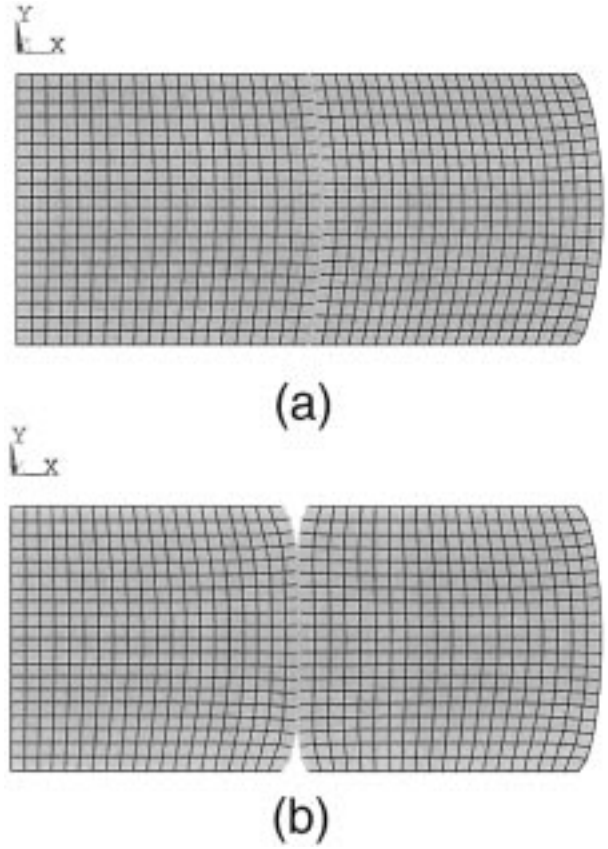

Figure 5 Deformed shape of the disk model with implant: (a) full size implant (same size as nucleus cavity), (b) small size implant (smaller than nucleus cavity). In both cases, the implant has a Young's modulus of 5 MPa. Friction between the implant and the end-plates is represented by total constraint of the nodes along the top and bottom edges of the implant area.

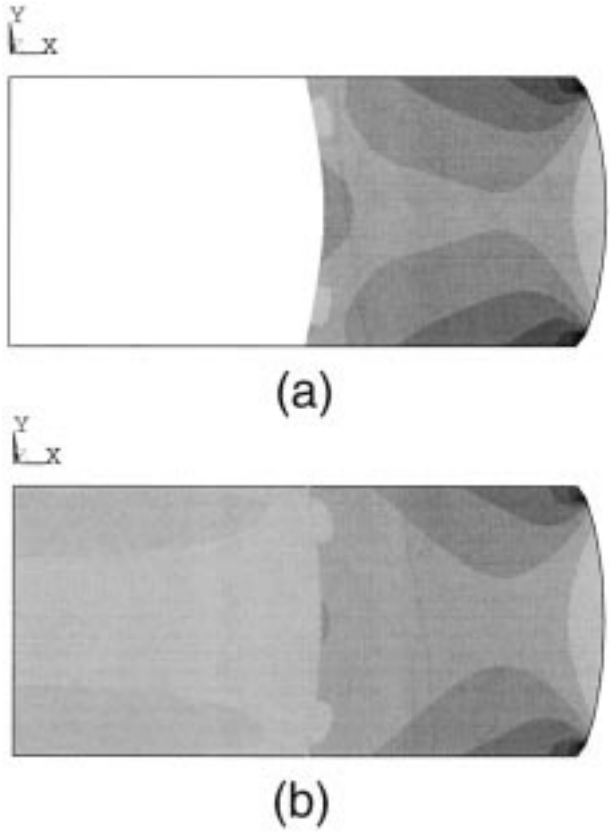

Figure 6 Distribution of von Mises stress: (a) intact disk, (b) disk with 3 MPa implant. The palest contour areas represent the lowest stresses and the darkest contour areas represent the highest stresses. The values of the stress contours are the same in both plots, but are not shown for the reasons given in the main text. Note that the intact disk nucleus in (a) is shown in white, as it was modeled as a fluid and hence von Mises stress is undefined in this region.

the implant does begin to push the annulus back out again. It was found that the degree of contact depended on the Young's modulus of the implant material. Also, although only one small size was considered, it can be deduced that the degree of contact will depend on the difference in size of the implant and the cavity.

The stress distribution in the annulus was used to determine which Young's modulus best reproduced the behavior of the intact disk. Fig. 6 shows the predicted distribution pattern of von Mises stress for the intact disk model (Fig. 6a) and an implant model with a Young's modulus of 3 MPa (Fig. 6b). The values of the contours in Fig. 6 are the same for each plot, with black representing high stresses, and the palest shade of gray representing low stresses. The numerical value for each contour is not given because, due to the number of simplifications and approximations in the model, the predicted stresses may not accurately represent the real stresses within a disk. However, comparison can still be made between the patterns of stress distribution produced by different implants and the intact disk model. Note that the nucleus of the intact disk (Fig. 6a) is shown in white as it is a fluid and hence von Mises stress is undefined in this region.

Comparison of Fig. 6b with 6a shows that an implant with a Young's modulus of 3 MPa gives a good match to the predicted pattern of von Mises stress in the annulus of the intact disk model. Since a good match was found at the lower end of the Young's modulus range tested in the model (0.5 to 100 MPa), the effects of having a much stiffer implant were also considered. Fig. 7 shows the stress distribution predicted for an implant with a Young's modulus of 100 MPa. The values of the stress contours in Fig. 7 are the same as in Fig. 6. It can be seen that the highest stresses (black regions) are concentrated in the implant. Within most of the annulus, the stresses are below those seen in the intact disk. This indicates that the applied load is mainly being supported by the implant and the annulus is being shielded from stress.

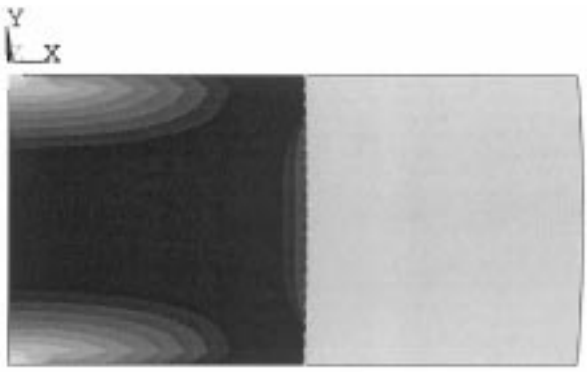

Figure 7 Distribution of von Mises stress in a disk with a 100 MPa implant. The contours have the same values as the plots in Fig. 6.

4. Discussion

A simple model of the intervertebral disk was developed and used to investigate the effects of removing and replacing the nucleus with a synthetic material, and to predict the ideal properties of such an implant. Although the model was simple, it allowed specific questions about the disk and a potential implant to be answered. The model was validated by comparing the predictions for the intact and denucleated disk with experimental results.

The model predicted that replacing the nucleus with a solid implant would push the annulus outwards under load, thus restoring the behavior of the intact disk. It also predicted that an implant smaller than the nucleus cavity was not as effective as a full size implant for reversing the changes caused by denucleation. The magnitude of axial displacement and bulging of the annulus margins depended on the Young's modulus of the implant. Stress distributions in the annulus with implants of different Young's modulus were compared with the stress distribution in the annulus of an intact disk. As a result, it was predicted that the most suitable implant material would have a Young's modulus of around 3 MPa since it led to a restoration of the normal stress distribution. Stiffer implants were seen to shield the annulus from stress. These results have implications for implant design.

Although not demonstrated in the results, it can be deduced that if load is being carried mainly by the implant, as was the case for stiffer implants, then this will result in high stresses in the underlying bone. If the stresses are greater than the strength of the bone, the implant could sink down into the vertebral body. Even if the stresses are lower than the bone strength, the changes in stress distribution may result in the remodeling of the vertebral body. This phenomena, described by Wolff's law, causes the bone to be restructured in response to mechanical stimulation, so that it becomes better adapted to support the new stresses [43]. Similarly, the predicted stress reduction in the annulus, produced by the shielding effect of a stiffer implant, may result in remodeling of the annulus tissue [44].

The predictions for small size implants, which do not fit perfectly into the nucleus cavity, also have implications for implant design. Several current implant designs consist of one or two blocks which are inserted into the nucleus cavity [45, 46]. If the gaps around the blocks are sufficiently large, then the implant will not be able to reverse the changes to the annulus behavior shown in this study. Although, the device of Ray *et al*. [46] is made out of a hydrophilic polymer, which swells in the presence of body fluids, its surrounding jacket is designed to limit expansion in the horizontal plane of the disk. Another implant design made out of similar material [47] is also specifically designed to have little sideways expansion. As predicted by the model, a better design is to have an implant which totally fills the nucleus cavity. One way to obtain this situation would be to inject the implant material into the disk such as is suggested by Bao *et al*. [48]. This would have the added advantage that the implant could be implanted using a minimally invasive surgical technique.

5. Conclusions

There were two major conclusions from this study. Firstly, replacement of the nucleus can reverse the changes in annulus behavior due to denucleation of the intervertebral disk. Secondly, suitable implants should fill the nucleus cavity and be soft with a Young's modulus of approximately 3 MPa.

Acknowledgments

We thank Dr K. J. Mathias for comments on the paper. We are also grateful to the Biotechnology and Biological Sciences Research Council and Smith and Nephew Group Research for funding this research.

References

1. D. W. L. HUKINS, in ''The Biology of the Intervertebral Disc'', volume 1, edited by P. Ghosh (CRC Press, Boca Raton, 1988) p. 1.
2. N. BOGDUK, in ''Clinical Anatomy of the Lumbar Spine'', 3rd edition (Churchill Livingstone, Melbourne, 1997) p. 13.
3. R. W. PORTER, in ''Management of Back Pain'', 2nd edition (Churchill Livingstone, Edinburgh, 1993) p. 180.
4. P. KAMBIN and H. GELLMAN, *Clin. Orthop.* **174** (1983) 127.
5. P. KAMBIN and L. ZHOU, *Clin. Orthop.* **337** (1997) 49.
6. D. S. J. CHOY, P. W. ASCHER, H. S. RANU, S. SADDEKNI, D. ALKAITIS, W. LIEBER, J. HUGHES, S. DIWAN and P. ALTMAN, *Spine* **17** (1992) 949.
7. D. WARDLAW, in ''Lumbar Spine Disorders: Current Concepts'', edited by R. M. Aspden and R. W. Porter (World Scientific, Singapore, 1995) p. 167.
8. E. SEROUSSI, M. H. KRAG, D. L. MULLER and M. H. POPE, *J. Orthop. Res.* **7** (1989) 122.
9. J. R. MEAKIN, Ph.D. thesis (University of Aberdeen, UK, 1999).
10. J. R. MEAKIN and D. W. L. HUKINS, *J. Bone Joint Surg.* **826** Suppl I (2000) 38.
11. V. K. GOEL, B.T. MONROE, L. G. GILBERTSON and P. BRINCKMANN, *Spine* **20** (1995) 689.
12. M. B. COVENTRY, R. K. GHORMLEY and J. W. KERNOHAN, *J. Bone Joint Surg.* **27** (1945) 233.
13. *Idem., ibid.* **27** (1945) 460.
14. C. D. RAY, in ''Clinical Efficacy and Outcome in the Diagnosis and Treatment of Low Back Pain'', edited by J. W. Weinstein (Raven Press, New York, 1992) p. 205.
15. T. BELYTSCHKO, R. F. KULAK and A. B. SCHULTZ, *J. Biomech.* **7** (1974) 277.
16. J. R. MEAKIN, R. M. ASPDEN and D. W. L. HUKINS, *Comments Theor. Biol.* **5** (1998) 49.
17. B. M. NIGG, in ''Biomechanics of the Musculo-skeletal System'', edited by B. M. Nigg and W. Herzog (John Wiley and Sons, Chichester, 1994) p. 367.
18. D. W. L. HUKINS. *Proc. R. Soc. Lond.* B **249** (1992) 281.
19. ANSYS ''Modelling and Meshing Guide'', 2nd edition (ANSYS Inc., Houston, PA, USA, 1997) p. 2.11.
20. ANSYS ''Elements Reference'' 9th edition, (ANSYS Inc., Houston, PA, USA, 1997).
21. J. S. POONI, BSc Thesis (University of Manchester, UK, 1983).
22. P. BRINCKMANN and H. GROOTENBOER, *Spine* **16** (1991) 641.
23. M. SHEA, T. Y. TAKEUCHI, R. H. WITTENBERG, A. A. WHITE III and W. C. HAYES, *J. Spinal Disord.* **7** (1994) 317.
24. H. YANG and V. L. KISH, *J. Biomech.* **21** (1988) 865.
25. J. M. GERE and S. P. TIMOSHENKO, ''Mechanics of Materials'', 2nd SI edition (Wadsworth International, Sydney, 1985) p. 21.
26. E. GOWER and V. PEDRINI, *J. Bone Joint Surg.* **51A** (1969) 1154.
27. G. LYONS, S. M. EISENSTEIN and M. B. E. SWEET, *Biochim. Biophys. Acta* **673** (1981) 443.
28. E. R. ACAROGLU, J. C. IATRIDIS, L. A. SETTON, R. J. FOSTER, V. C. MOW and M. WEIDENBAUM, *Spine* **20** (1995) 2690.

29. C. WU and R. F. YAO, *J. Biomech.* **9** (1976) 1.
30. F. MARCHAND and A. M. AHMED, *Trans. Orthop. Res. Soc.* **14** (1989) 355.
31. B. A. BEST, F. GUILAK, L. A. SETTON, W. ZHU, F. SAED-NEJAD, A. RATCLIFFE, M. WEIDENBAUM and V. C. MOW, *Spine* **19** (1994) 212.
32. L. SKAGGS, M. WEIDENBAUM, J. C. IATRIDIS, A. RATCLIFFE and V. C. MOW, *ibid.* **19** (1994) 1310.
33. S. EBARA, J. C. IATRIDIS, L. A. SETTON, R. J. FOSTER, V. C. MOW and M. WEIDENBAUM, *ibid.* **21** (1996) 452.
34. S. UMEHARA, S. TADANO, K. ABUMI, K. KATAGIRI, K. KANEDA and T. UKAI, *ibid.* **21** (1996) 811.
35. M. A. ADAMS and T. P. GREEN, *Eur. Spine J.* **2** (1993) 203.
36. A. D. HOLMES, D. W. L. HUKINS and A. J. FREEMONT, *Spine* **18** (1993) 128.
37. W. J. VIRGIN, *J. Bone Joint Surg.* **33B** (1951) 607.
38. T. BROWN, R. J. HANSEN and A. J. YORRA, *ibid* **39A** (1957) 1135.
39. K. L. MARKOLF, *J. Bone Joint Surg.* **54A** (1972) 511.
40. K. H. WENGER and J. D. SCHLEGEL, *Clin. Biomech.* **12** (1997) 438.
41. K. L. MARKOLF and J. M. MORRIS, *J. Bone Joint Surg.* **54A** (1974) 511.
42. J. VINCENT ''Structural Biomaterials'', revised edition (Princeton University Press, Princeton, 1990) p. 101.
43. J. B. PARK and R. S. LAKES ''Biomaterials: An Introduction'', 2nd edition (Plenum Press, New York, 1992) p. 221.
44. D. BRICKLEY-PARSONS and M. J. GLIMCHER, *Spine* **9** (1984) 148.
45. J. D. KUNTZ, ''Intervertebral Disc Prosthesis'' (US patent number 434 9922, 1982).
46. C. D. RAY, E. A. DICKHUDT, P. J. LEDOUX and B. A. FRUTIGER, ''Prosthetic Spinal Disc Nucleus'' (US patent number 567 4295, 1997).
47. Q.-B. BAO and P. A. HIGHAM, ''Hydrogel Intervertebral Disc Nucleus with Diminished Lateral Bulging'' (US patent number 553 4028, 1996).
48. Q.-B. BAO, P. A. HIGHAM, C. S. BAGGA and H. A. YUAN, ''Method and apparatus for injecting an elastic spinal implant'' (US patent number 580 0549, 1998).

Received 9 June
and accepted 14 December 1999